
Surface characteristics and dissolution behavior of plasma-sprayed hydroxyapatite coating

Limin Sun,¹ Christopher C. Berndt,¹ Khiam Aik Khor,² H. N. Cheang,² Karlis A. Gross³

¹Center for Thermal Spray Research, State University of New York at Stony Brook, 306 Old Engineering, Stony Brook, New York 11794-2275

²Advanced Materials Research Centre (AMRC), Nanyang Technological University, 639798 Singapore

³School of Physics and Materials Engineering, Monash University, Victoria 3800 Australia

Received 21 November 2001; revised 18 February 2002; accepted 27 February 2002

Published online 1 August 2002 in Wiley InterScience (www.interscience.wiley.com). DOI: 10.1002/jbm.10315

Abstract: One of the most important concerns with the clinical use of plasma-sprayed hydroxyapatite (HA) coatings is the resorption of the coating, and dissolution at neutral pH is one of the two major resorption mechanisms. In this study, highly crystalline pure HA powders were atmospherically plasma sprayed using various parameters. Dissolution of both HA powders and coatings was measured using a calcium ion meter. Surface characteristics, including phase, morphology, and roughness, were compared for the coatings before and after dissolution. Pulverized HA coatings exhibited significantly higher dissolution compared with the same quantity of feedstock HA powders because of the decreased crystallinity and fine crystal size of the coating. Furthermore, the dissolution decreased with the crystallinity of the coating. Dissolution of HA coatings did not show much difference with respect to the coatings in the initial stage of immersion (4 h). However, dissolution of all coatings reached saturation in a fresh physiological solution. The saturation values were much lower compared with their counterparts in the form of powders, which may imply the stability of HA coatings in long-term use. In addition to crystallinity, the particle melting status in the coatings, i.e.,

the volume of nanocrystals, and porosity, was found to be another important factor for the dissolution of the HA coating. X-ray diffraction patterns of HA coatings indicated the complete dissolution of impurity phases and amorphous phase after the coatings were immersed in the solution for 4 days. Coatings sprayed at lower power (27.5 kW) exhibited a pattern of crystalline HA whereas coatings sprayed at higher power (42 kW) exhibited a pattern of bone apatite. Surface morphologies showed preferential dissolution of amorphous phase in all coatings accompanied with precipitation of bone apatite observable for coatings sprayed at higher power. Surface roughness measured after the dissolution studies increased for the two coatings sprayed at lower power level but decreased for coatings sprayed at higher power level. This decrease is attributed to the better match in solubility characteristics between the fine crystals and the amorphous calcium phosphate within the coating. © 2002 Wiley Periodicals, Inc. *J Biomed Mater Res* 62: 228–236, 2002

Key words: hydroxyapatite; plasma-sprayed coating; crystallinity; dissolution; particle melting status

INTRODUCTION

A prerequisite for an orthopedic or dental prosthesis to function properly is permanent fixation to the skeletal system. A successful fixation should be fast and strong initially and exhibit lifelong stability. Several fixation methods have been used for the current prostheses, including both cemented fixation,¹ and cementless fixation; three examples of the

latter method are a press-fit, the use of a porous surface,^{3,4} and a plasma-sprayed hydroxyapatite (HA) [Ca₁₀(PO₄)₆(OH)₂] coating.^{5–7} Compared with other methods, the use of HA coating exhibits a more rapid fixation and stronger bonding between the host bone and the implant, as well as increased uniform bone ingrowth and/or ongrowth at the bone–implant interface.^{8–10} However, there are still many concerns about the use of HA coatings, especially with regard to durability. One important concern is the resorption of HA coatings in a biological environment, which could lead to coating disintegration, resulting in the loss of both bond strength and implant fixation as well as the threat of formation of particulate debris.^{11,12}

Six resorption mechanisms have been hypothesized by Bauer¹³ and Gross et al.,^{14,15} but generally only two

Correspondence to: C. C. Berndt; e-mail: cberndt@notes.cc.sunysb.edu

Contract grant sponsor: NSF-MRSEC DMR; contract grant number: 9632570

of them concern the clinical use of HA coatings, i.e., (1) dissolution at neutral pH, and (2) osteoclastic resorption of the coating as part of normal bone remodeling. Dissolution is an important variable and can be affected by the characteristics of both the HA coating and physiological solution. The critical coating specifications include purity (phase composition), crystallinity, Ca/P ratio, microstructure, porosity, surface morphology and roughness, thickness, and implant type and surface texture, which also lead to different mechanical properties. Most of these variables result from different processing parameters and can lead to different dissolution and subsequent precipitation. For example, all new phases in the HA coating, including amorphous calcium-phosphate (ACP), tricalcium phosphate [$\text{Ca}_3(\text{PO}_4)_2$], α -TCP and β -TCP], tetracalcium phosphate ($\text{Ca}_4\text{P}_2\text{O}_9$, TTCP), oxyhydroxyapatite [$\text{Ca}_{10}(\text{PO}_4)_6(\text{OH})_{2-2x}(\text{O})_x(\square)_x$, OHA, where \square represents a vacancy] and calcium oxide (CaO), have much higher dissolution than the crystalline HA.^{16,17} Partial dissolution of the HA coating is essential to trigger bone growth, but exceedingly rapid dissolution leads to poor bone bonding and coating disintegration. Therefore, it is important to optimally control the coating characteristics by varying the processing conditions. As well, the characteristics and properties of the HA coating will be changed after different degrees of dissolution, which will affect the clinical performance.

Among all coating characteristics, the coating surface is especially crucial for the fixation mechanism, because it is in direct contact with the bone and body fluid on implantation. In the present study, we investigated the dissolution behavior of HA coatings sprayed under different conditions and compared the surface characteristics of HA coatings before and after dissolution, with the aim to explore the relationship between spraying parameters, coating characteristics, and dissolution. It is generally believed that an amorphous coating has higher dissolution than a crystalline coating, i.e., crystallinity is the dominant factor for the dissolution of the HA coating. However, other studies found little difference in the dissolution between amorphous and crystalline coatings or even opposite results.^{18,19} In contrast to the previous studies,^{18,19} which investigated only the relationship between coating characteristics (usually crystallinity) and dissolution, the present study also included the information of spraying parameters so that the effects of other coating characteristics such as particle melting status, i.e., volume of nanocrystals, and porosity could be considered. In addition, the physiological solution for immersing the coating was refreshed in the middle of the experiment (after 1 day) and the dissolution measurement was repeated after a long immersion time (after 3 days) to simulate the metabolic physiological environment around implants.

EXPERIMENTAL

Feedstock and plasma spraying

The feedstock was calcined spray-dried HA powders provided by AMRC, Nanyang Technological University of Singapore.^{20,21} The powders were fully crystalline pure HA phase and were sieved to less than 100 μm before spraying to ensure uniform melting and deposition. The feedstock was then atmospherically plasma sprayed using a Metco 3MB plasma torch with a GH nozzle (Sulzer-Metco, Westbury, NY). Argon was used as both the primary gas (at 50 slpm) and carrier gas (at 3.65 slpm), and hydrogen (at a variable level to attain certain power levels) as the secondary gas. Two types of spray power and two stand off distances (SOD) were selected (Table I). Immediately before spraying, the stainless steel substrate was (1) grit blasted using Al_2O_3 grit, and (2) cleaned with acetone.

Dissolution testing

Bioactivity can be assessed from the rate and volume of dissolution and formation of a carbonated apatite layer. The bioactivity of the feedstock HA powders and coatings was evaluated with a PHM250 ion analyzer (Radiometer, Copenhagen, Denmark) and a calcium ion specific electrode calibrated using 400, 40, 4, and 0.4 ppm standard solutions prepared from $\text{CaCl}_2 \cdot 2\text{H}_2\text{O}$ at 37°C. The test sample was 25-mg powder lots (feedstock powders or powders pulverized from peel-off coatings) or 15 × 15 mm coatings deposited onto stainless steel substrates. The edges of the coatings were sealed using a neutral curing silicone sealant and dried in air for 48 h. The release of calcium ions was ascertained in 50 mL of 0.1M tris-(hydroxymethyl)-aminomethane buffered with HCl to pH = 7.3 (contained in a vial of 36-mm diameter and 70-mm height) at ~37°C for up to 4 h. The solution for the coating was refreshed after 1 day and the measurement was repeated for the same coating after another 2 days' immersion in the new solution. A homogeneous solution was maintained during measurement

TABLE I
Plasma-Spray Parameters

Sample Type	Spray Current (A)	Spray Voltage (V)	Secondary Gas (H_2 , slm)	Spray Power (kW)	Stand-Off Distance (mm)
B1	500	55	5.6	27.5	80
B2	500	55	5.6	27.5	160
B5	600	70	11	42	80
B6	600	70	11	42	160

by stirring (using a three-blade stirrer with a blade length of 9 mm) at 300 rpm. The samples were then removed after another day of immersion and dried in air for subsequent surface characterization.

Surface characterization

X-ray diffraction (XRD) was performed on both feedstock HA powders and coating surfaces before and after dissolution using a computer-controlled Philips PW 1729 X-ray diffractometer with $\text{CuK}\alpha_1$ radiation at 40 kV and 30 mA. The goniometer was set at a scan speed of $0.005^\circ/\text{s}$, a step size of 0.02, over a 2θ range of $20\text{--}60^\circ$. The crystallinity of the HA coating was determined from the XRD pattern using the following equation^{22,23}:

$$\text{Crystallinity (\%)} = \frac{A_C}{A_C + A_A} \times 100\% \quad (1)$$

where A_C is the total integrated intensity of all HA peaks within $25\text{--}37^\circ$. It is calculated by multiplying the area of the most intense (211) peak of HA by 3.23, which is the ratio of the total intensity of all HA peaks within $25\text{--}37^\circ$ in JCPDS (Joint Committee on Powder Diffraction Standard) card (9-432) to the intensity of the (211) peak. The term A_A is the integrated intensity of the ACP phase, which was evaluated using the area of the amorphous hump between 25 and 37° . All peak area calculations were performed using curve fitting and the error was estimated to be around $\pm 2\%$ of the mean value.

The morphologies of HA powders and coating surfaces before and after dissolution were examined using a Philips ISI-SX-30 scanning electron microscope. The surface roughness (R_a) of the HA coating was measured using a Zygo New View 200 non-contact surface profiler (Zygo Co., Middlefield, CT), which is a scanning white-light interferometer. The average of three measurements is reported.

RESULTS AND DISCUSSION

Feedstock characterization

The morphology of the feedstock HA powders (Fig. 1) shows that all particles are rounded, and each particle is the agglomerate of many fine particles (particle size $< 1\ \mu\text{m}$) that create a rough surface.

Surface characteristics of as-sprayed HA coatings

The XRD patterns of HA coatings in the as-sprayed state are shown in Figure 2 (i.e., before dissolution). At

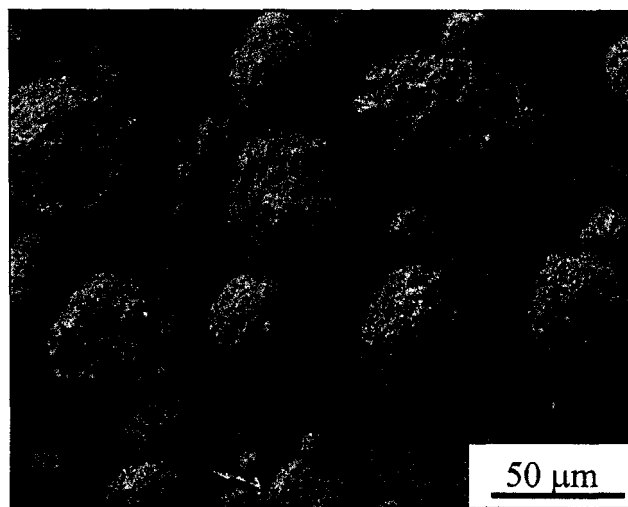


Figure 1. Scanning electron microscope morphology of feedstock HA powders.

the same SOD, when the spray power increased from 27.5 to 42 kW (B1 \rightarrow B5, B2 \rightarrow B6), the amorphous hump became more obvious, i.e., the crystallinity decreased (Fig. 3). This response arises because an increase in power causes a higher plasma temperature and, thus, a higher fraction of powder is likely to melt. Therefore, more ACP will form from the melt as a result of the rapid cooling rate of the spray process. Meanwhile, the increased cooling rate and dehydroxylation also promoted the formation of ACP. At the same spray power, when the SOD increased from 80 to 160 mm (B1 \rightarrow B2, B5 \rightarrow B6), the amorphous hump (at $2\theta = 25\text{--}37^\circ$) became significant, i.e., the crystallinity decreased (Fig. 3). Such behavior occurs from a higher melted fraction and accompanying dehydroxylation of the particles during transport in the plasma. In addition to the ACP, the peaks of all impurity phases (α -TCP, β -TCP, TTCP, and CaO) increased with an increase in either spray power or SOD. The reasons could be that: (1) HA powders suffered more melting, decomposition, and dehydroxylation in both cases, and (2) some of the crystalline HA transformed to ACP.^{24,25} The surface morphologies of as-sprayed HA coatings are shown in Figure 4. The morphology of the coating sprayed at 27.5 kW and 80 mm (B1) was dominated by unmelted and partially melted particles over a small proportion of flattened splats. These particles were either quite large with a partially melted skin or were disintegrated into fine particles. This result is consistent with the XRD result because this coating exhibits the highest crystallinity ($\sim 86.5\%$). When the SOD increased to 160 mm (B2), the morphology was mainly composed of glassy phases, including flattened splats, accumulated splats, and spheroidized particles, despite the remains of some unmelted fine particles. The particles displayed a higher degree of melting for the two coat-

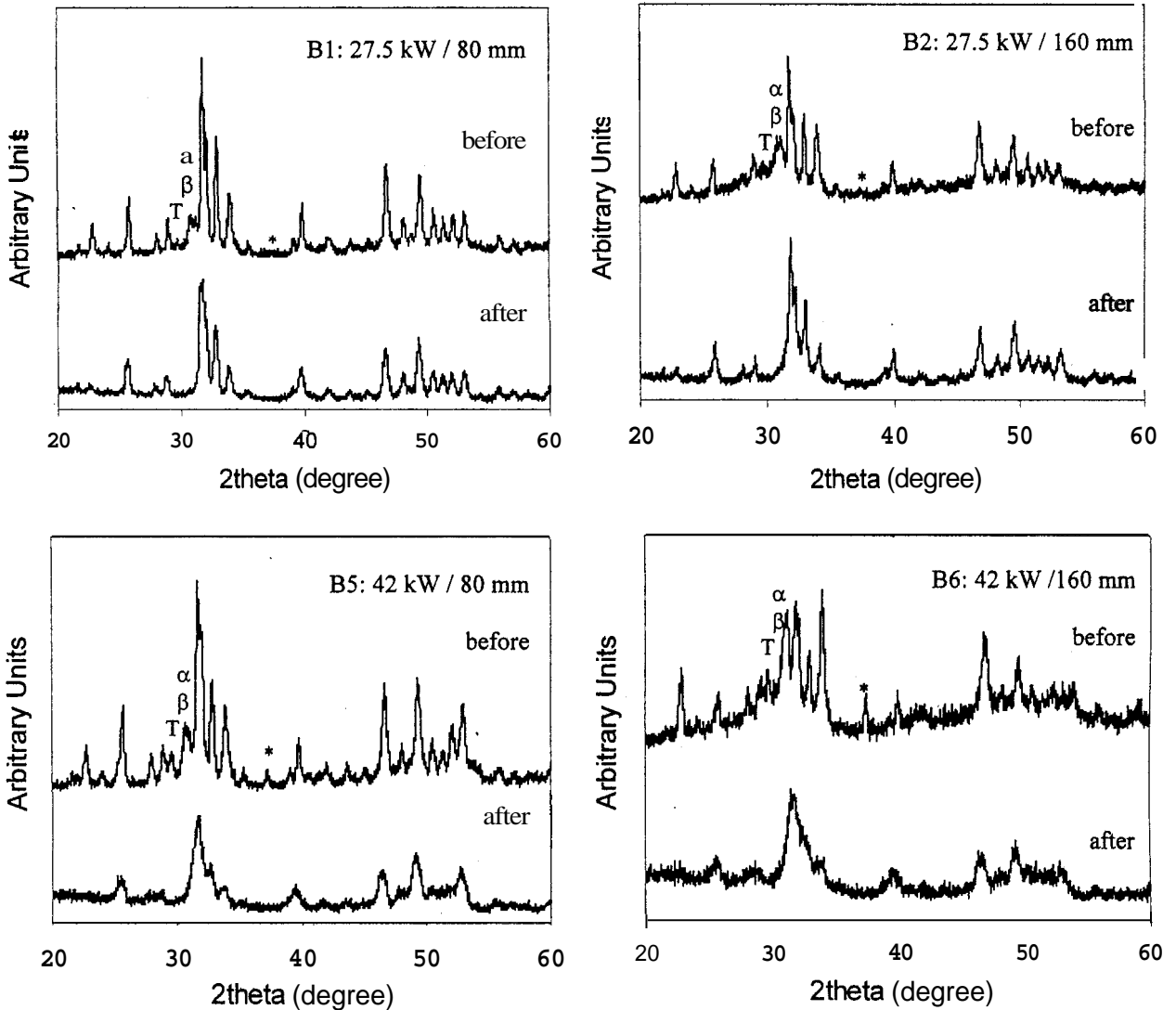


Figure 2. XRD patterns of HA coatings before (as-sprayed) and after dissolution, a, α -TCP; β , β -TCP, T, TTCP; *, CaO. All other peaks belong to HA.

ings sprayed at 42 kW. The coating sprayed at 80 mm (B5) consisted mainly of flattened and accumulated splats as well as some spheroidized and partially melted fine particles. For the coating sprayed at 160 mm (B6), almost all particles were melted and the major morphological artifacts were flattened and accumulated glassy splats as well as some spheroidized particles.

The surface roughness of the HA coatings reflects the irregular morphology of the coating surface. Coatings B2 and B6, which revealed a lower crystallinity, exhibited a rougher surface in the as-sprayed state arising from respheroidized droplets deposited onto the surface during coating generation (Fig. 5).

Dissolution

The pulverized HA coatings exhibited much higher dissolution than the feedstock [Fig. 6(a)]. This can be

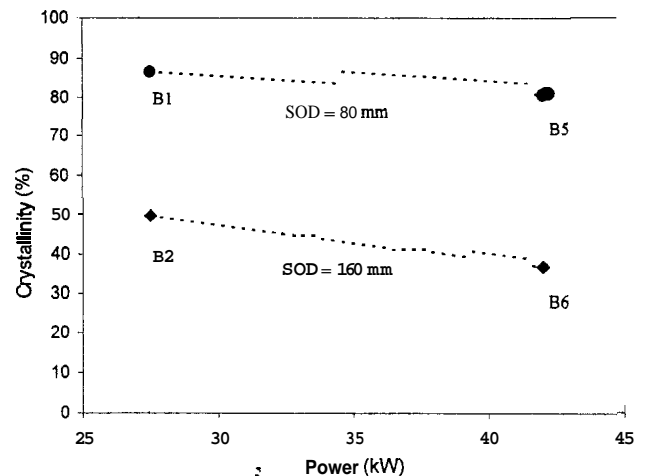


Figure 3. Crystallinity of HA coatings sprayed at different powers and SOD.

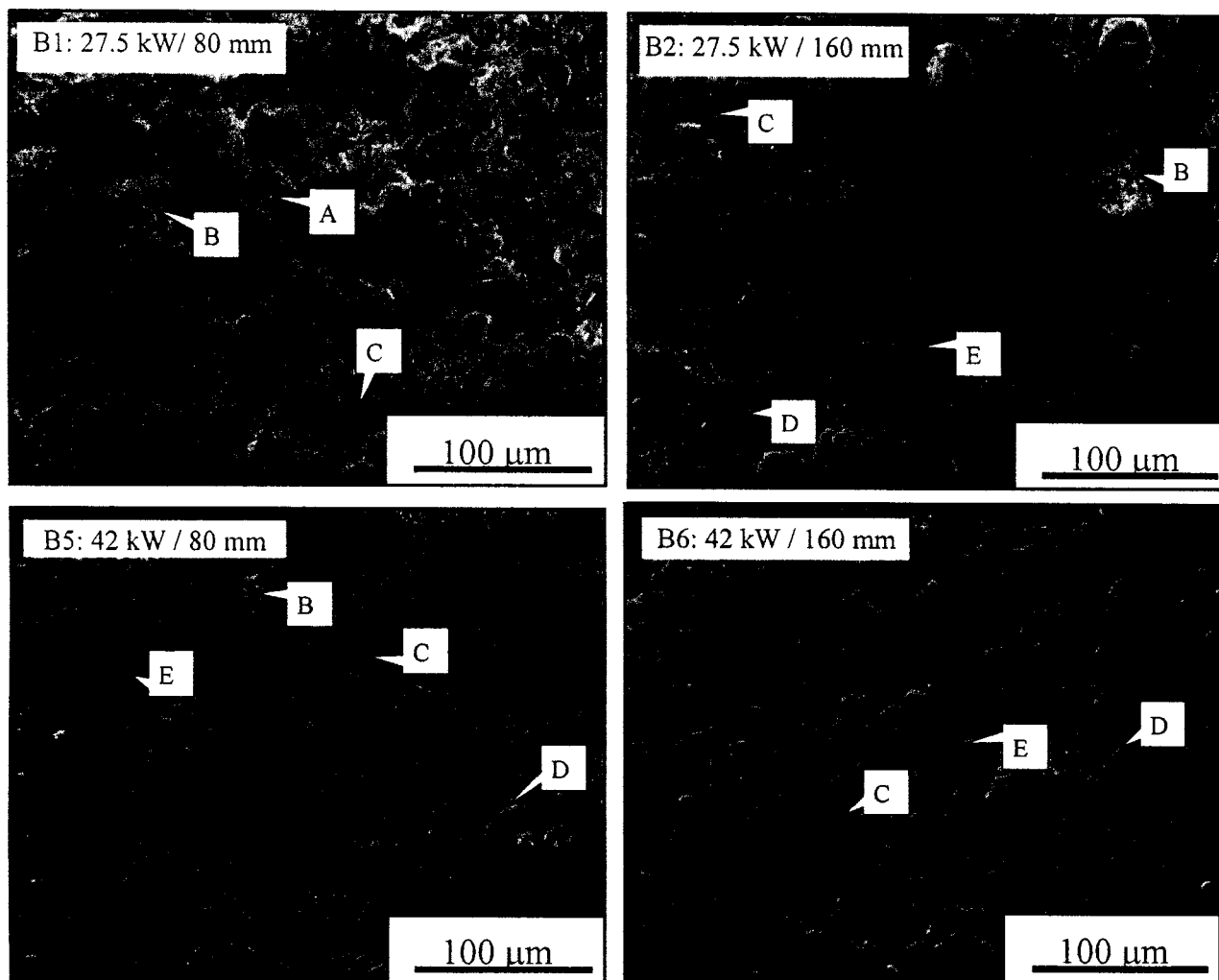


Figure 4. Surface morphologies of as-sprayed HA coatings. A, partially melted large particle; B, partially melted fine particle; C, flattened splat; D, accumulated splat; E, spheroidized particle.

explained by the phase composition and the smaller crystal size in the plasma-sprayed HA coating.^{26,27} As discussed previously, both crystallinity and purity of HA decreased after spraying and all new phases had

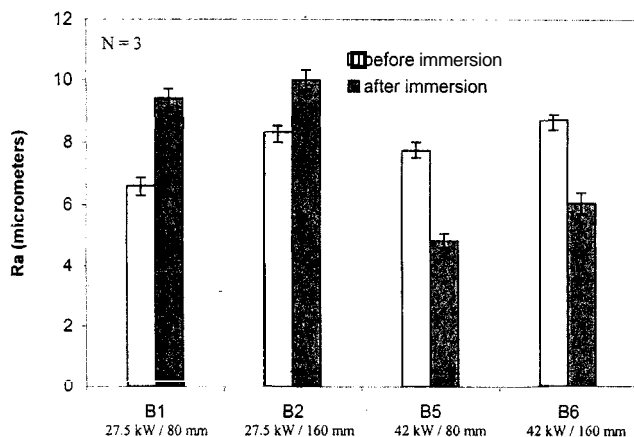


Figure 5. Surface roughness of HA coatings before and after dissolution. N, number of measurements.

significantly higher dissolution than HA.^{16,17} Thus, it would be expected that coatings with lower crystallinity (B2, B6) would exhibit higher dissolution because the amorphous phase has a much higher dissolution than all other phases and is, therefore, the dominant factor.

The dissolution of the as-sprayed HA coatings in the initial immersion stage [Fig. 6(b)], however, shows little difference between coatings despite slightly higher values for the low-crystallinity coatings (B2, B6). Unlike powders, dissolution of coatings are not only decided by the phase composition and crystal size, but also by other coating characteristics, such as morphology, roughness, surface area, porosity, and residual stress. As a matter of fact, all properties of thermal-sprayed coatings are influenced by such feature. Dissolution for coatings in the initial immersion stage were the balance of many factors, but were not dominated by the crystallinity as was the case for the pulverized coatings.

An interesting finding concerns the dissolution of

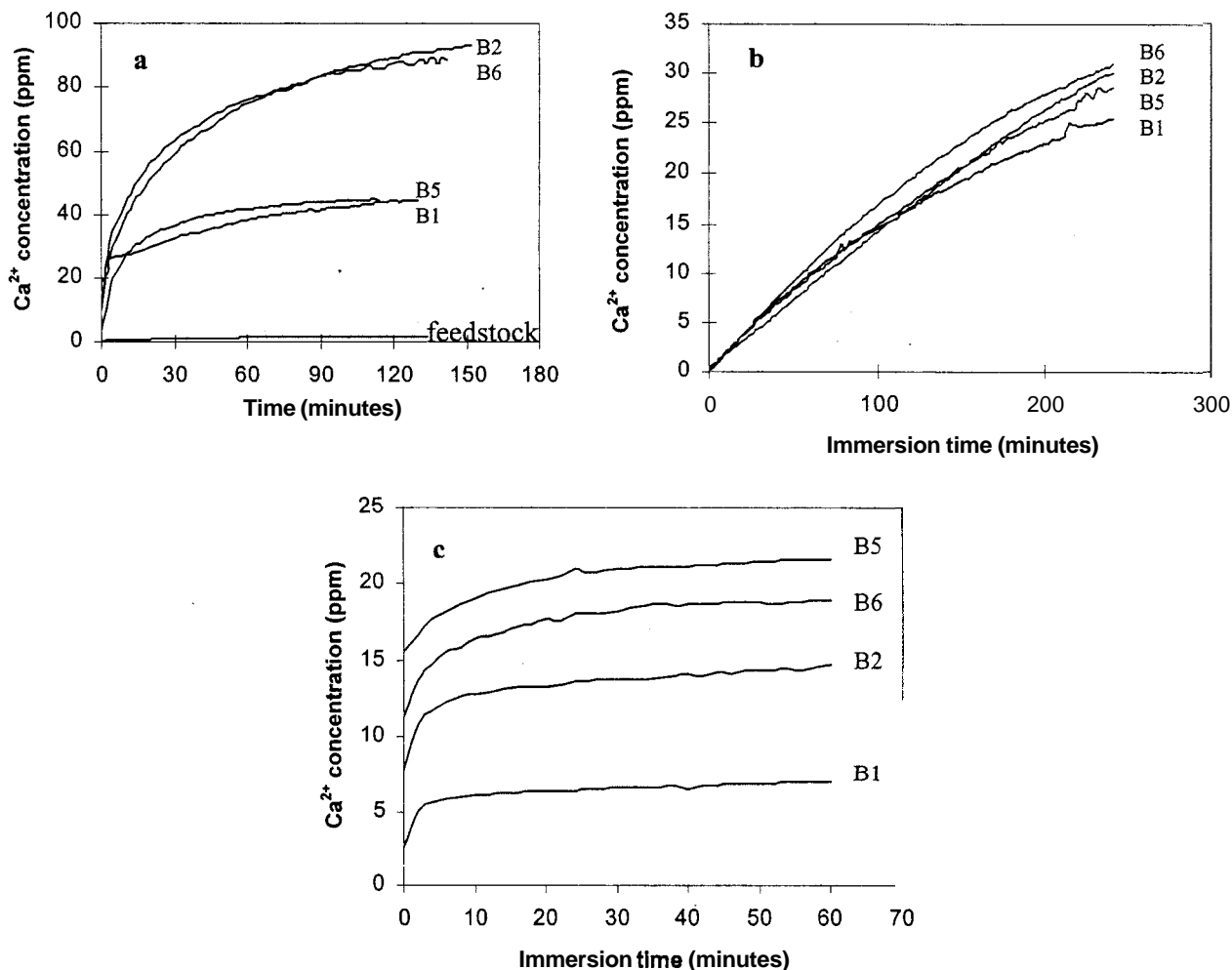


Figure 6. Dissolution rates of (a) feedstock HA powders and powders pulverized from HA coatings; (b) as-sprayed HA coatings; and (c) HA coatings after 3 days' immersion. B1, 27.5 kW/80 mm; B2, 27.5 kW/160 mm; B5, 42 kW/80 mm; B6, 42 kW/160 mm.

the coatings after 3 days of immersion [Fig. 6(c)]. The Ca²⁺ concentrations almost stabilized for all four coatings within 60 min (B1, 7 ppm; B2, 14 ppm; B5, 21 ppm; B6, 19 ppm). It should be noted that the solution was refreshed after the first day of immersion. The low value is reasonable because most amorphous and impurity phases have dissolved in the first solution. This suggests a change to a more stable HA coating for long-term use after initial dissolution.

As is well known, because of the extremely high temperature of the plasma flame, HA powders could be entirely or partially melted during the spray process. Whereas the unmelted portions typically retain their crystalline structure after cooling, the melt could either become amorphous phase or recrystallize to nanocrystals according to the different cooling rates. It has been suggested that the amorphous phase is metastable and possesses a higher internal energy and tends to release the distortion.^{19,30} Therefore, the amorphous phase exhibits a higher dissolution compared with the crystalline HA phase when immersed

in solution. Nanocrystals, although in a stable state, have much greater interfacial volume as well as point defects from the rapid crystallization, which could lead to higher dissolution compared with the feedstock HA crystallites.

In Figure 6(c), coating B1 presents the lowest dissolution because it is the most crystalline one and the crystalline component is composed of a large fraction of the unmelted part of particles (Fig. 4). The large grain size transferred from the unmelted component of particles will, thus, lead to a lower solubility. For coating B2, despite the remains of some unmelted part of particles, the crystalline HA component is mostly composed of the nanocrystalline HA from recrystallization during spraying, which has higher solubility than the unmelted HA component; therefore, it has a higher saturation value than B1. For the same reason, coatings B5 and B6, in which the crystalline HA component is almost all nanocrystalline HA, exhibit even higher saturation values. The higher porosity for coating B5 (~7%), as compared with coating B2 (~5%) and

B6 (~3%), may contribute to the highest saturation value for this coating because of higher contact areas with the solution. Therefore, in addition to the amorphous phase, the particle melting status, i.e., volume of nanocrystals, and the porosity, could be important factors for the dissolution and resorption of HA coatings in long-term use. It should be noted that the saturation values could also be related to the disturbance (because of restirring during measurement) of the equilibrium condition of precipitated apatite, as indicated below. Nonetheless, dissolution of the HA coating is a complex process that involves many physical, chemical, and physiological factors.^{15,22} To further understand the process, one technique is to study the effects of the dissolution on the coating characteristics.

Surface characteristics of HA coatings after dissolution

The XRD patterns of the HA coatings indicate that no impurity phases were observed after dissolution

(Fig. 2). The two coatings sprayed at a lower power level (B1, B2) exhibit a pattern of crystalline HA that indicates the total dissolution of the amorphous phase from the surface of the coating. The slight increase in peak width is indicative of a small amount of precipitated apatite.³¹ The wide peak width superimposed onto the more intense narrow peaks produce a small but noticeable difference in peak shape. The two coatings sprayed at higher power level (B5, B6) show a pattern more similar to that of bone apatite, which is usually due to apatite precipitation on the coating.^{19,32,33} These results are consistent with the dissolution results. The release of Ca^{2+} and PO_4^{-3} ions occurs at a high concentration and is then precipitated on the coating to form a bone-like apatite. This behavior was verified by the surface morphology of HA coatings after dissolution (Fig. 7).

The morphologies of the two amorphous coatings (B2, B6) exhibit a microstructurally "rough surface instead of the original smooth glassy phase after dissolution, which indicated the preferential dissolution of amorphous phase. The coating with highest crys-

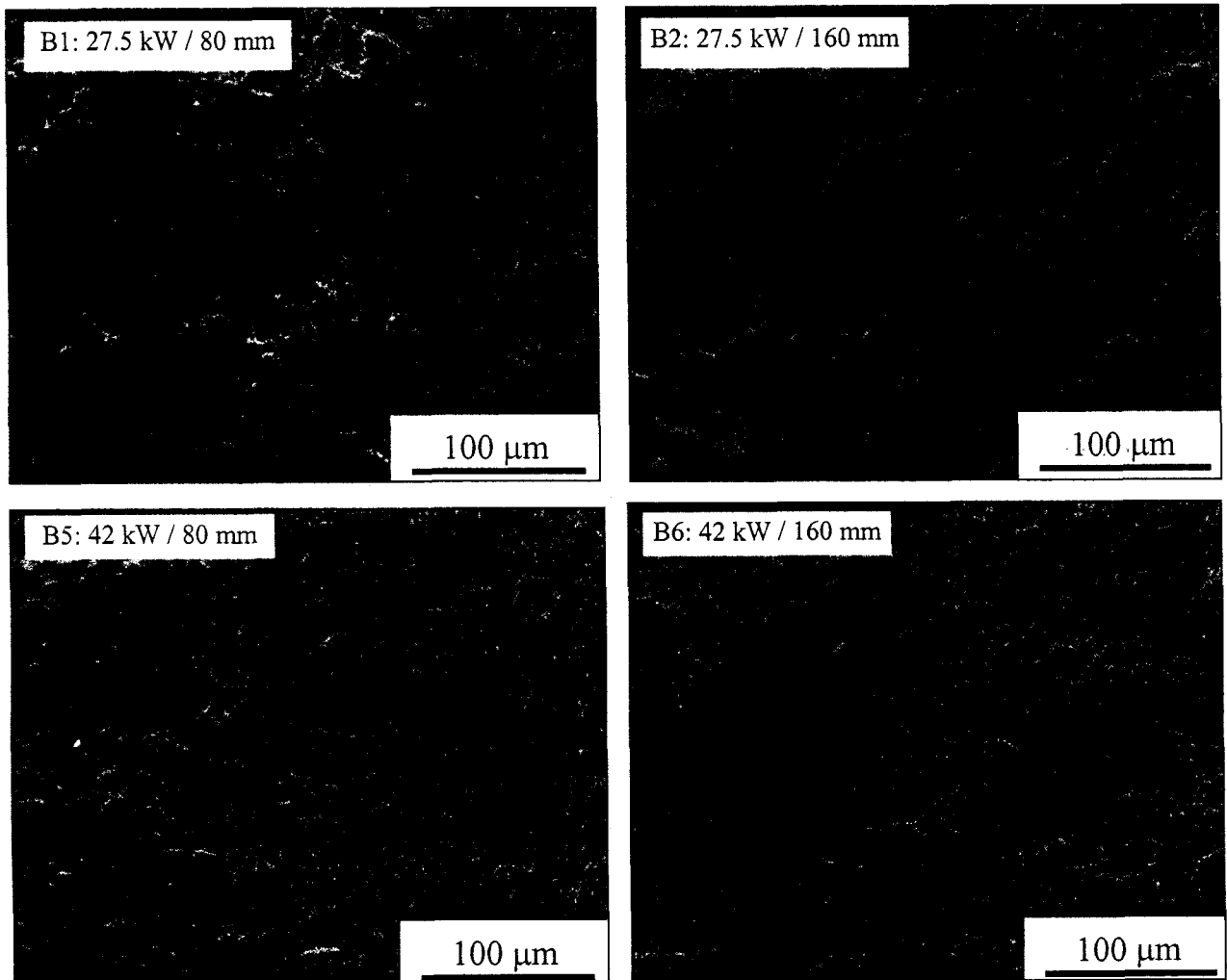


Figure 7. Surface morphologies of HA coatings after dissolution.

tallinity (B1) also exhibited indications of dissolution with the partially melted powders becoming smaller because of the dissolution of the outer melted layer of the deposited particles. For the two coatings sprayed at higher power (B5, B6), some fine particles could be observed on the surface, which are probably the precipitated apatite and can explain the bone apatite-like XRD patterns for these two coatings. The results also imply that particle melting status, or the existence of nanocrystals is more important than the amorphous phase for the nucleation and precipitation of bone apatite³⁴ despite a higher dissolution of the amorphous phase.

The roughness of the two coatings sprayed at lower power (B1, B2) became higher after dissolution whereas the opposite effect was observed for the two coatings sprayed at higher power (B5, B6). It is likely that the preferential dissolution of amorphous and impurity phases increased the roughness in the former case, whereas two factors were responsible for the smoother coating in the latter case. First, the degree of solubility was more closely matched between the fine crystals and the ACP within the coating. Second, the precipitation of apatite in the depressions and pores exposed to the physiological solution, where a relatively steady supersaturation can be maintained for heterogeneous nucleation,¹⁹ can lead to a smoother coating.

CONCLUSIONS

The relationship between spraying parameters, surface characteristics, and dissolution of HA coatings was investigated, and the following conclusions can be made.

1. The crystallinity and purity of HA decreased with increasing spray power and spray distance. Surface morphology of the coating sprayed at higher power and longer spray distance revealed much better particle melting.
2. HA coatings in the form of powders exhibit much higher dissolution compared with the feedstock powders and the coating. This is attributed to the finer crystal size and the higher surface area. Dissolution of different HA coatings did not show much difference during the initial stage of immersion (4 h), but all reached saturation in the fresh solution. The low saturation values (compared with their counterparts in the form of powders) indicated the stability of HA coatings in long-term use. The dissolution of the HA coating was affected not only by the crystallinity, but also by the particle melting status in the coatings, i.e., the volume of nanocrystals, and porosity.
3. XRD patterns of HA coatings showed the complete dissolution of impurity phases and amorphous phase after immersion in physiological solution for 4 days. Coatings sprayed at a lower power level exhibited a pattern of crystalline HA whereas coatings sprayed at a higher power level exhibited a pattern of bone apatite. Surface morphologies showed preferential dissolution of amorphous phase in all coatings and precipitation of apatite at a noticeable level for the coatings sprayed at higher power. Surface roughness increased for coatings sprayed at a lower power and decreased for coatings sprayed at a higher power.

The authors thank Matthew R. Gold and Dr. Rogerio S. Lima for their help. The ion analyzer was funded by the Ramaciotti Foundation awarded to K. A. G.

References

1. Galante JO, Jacobs J. Clinical performance of ingrowth surfaces. *Clin Orthop* 1992;276:41-49.
2. Hulbert SF, Cook SD. The case of a composite hip prosthesis. In: Vincenzini P, editor. *Ceramics in substitutive and reconstructive surgery*. New York: Elsevier Science Publishers; 1991. p 545-565.
3. Bloebaum RD, Mihalopoulos NL, Jensen JW, Dorr LD. Post-mortem analysis of bone growth into porous-coated acetabular components. *J Bone Joint Surg* 1997;79-A:1013-1022.
4. Pidhorz LE, Urban RM, Jacobs JJ, Sumner DR, Galante JO. A quantitative study of bone and soft tissues in cementless porous-coated acetabular components retrieved at autopsy. *J Arthroplasty* 1993;8:213-225.
5. Capello WD, D'Antonio JA, Feinberg JR, Manley MT. Hydroxyapatite-coated total hip femoral components in patients less than 50 years old: Clinical and radiographic results after 5 to 8 years of follow-up. *J Bone Joint Surg* 1997;79-A(7):1023-1029.
6. Soballe K, Hansen ES, Rasmussen HB, et al. Gap healing enhanced by hydroxyapatite coatings in dogs. *Clin Orthop* 1991; 272:300-307.
7. Soballe K, Hansen ES, Rasmussen HB, Bunger C. Tissue ingrowth into titanium and hydroxyapatite coated implants during stable and unstable mechanical conditions. *J Orthop Res* 1992;10:285-299.
8. Geesink RGT, de Groot K, Klein CP. Bonding of bone to apatite-coated implants. *J Bone Joint Surg* 1988;70-B:17-21.
9. Cook SD, Thomas KA, Dalton JF, Volkman TK, Whitecloud TS III, Kay JF. Hydroxyapatite coating of porous implants improves bone ingrowth and interface attachment strength. *J Biomed Mater Res* 1992;26:989-1001.
10. Stephenson PK, Freeman MA, Revell PA, Germain J, Tuke M, Pirie CJ. The effect of hydroxyapatite coating on ingrowth of bone into cavities in an implant. *J Arthroplasty* 1991;6:51-58.
11. Bauer TW, Geesink RCT, Zimmerman R, McMahon JT. Hydroxyapatite-coated femoral stems: Histological analysis of components retrieved at autopsy. *J Bone Joint Surg* 1991;73-A(12):1439-1452.
12. Collier JP, Surprenant VA, Mayor MB, Wrona M, Jensen RE, Surprenant HP. Loss of hydroxyapatite coating on retrieved, total hip components. *J Arthroplasty* 1993;8:389-393.

13. Bauer TW. Hydroxyapatite: Coating controversies. *Orthopedics* 1995;18(9):885-888.
14. Gross KA, Ray N, Røkkum M. The contribution of coating microstructure to degradation and particle release in hydroxyapatite coated prostheses. *J Biomed Mater Res*. To appear.
15. Sun L, Berndt CC, Gross KA, Kucuk A. Materials fundamentals and clinical performance of plasma sprayed hydroxyapatite coatings. *J Biomed Mater Res* 2001;58(5):570-592.
16. Radin SR, Ducheyne P. Plasma spraying induced changes of calcium phosphate ceramic characteristics and the effect on *in vitro* stability. *J Mater Sci Mater Med* 1992;3:33-42.
17. LeGeros RZ. Biodegradation and bioresorption of calcium phosphate ceramics. *Clin Mater* 1993;14:65-68.
18. Maxian SH, Zawadsky JP, Dunn MG. *In vitro* evaluation of amorphous calcium phosphate and poorly crystallized hydroxyapatite coatings on titanium implants. *J Biomed Mater Res* 1993;27:111-117.
19. Weng J, Liu Q, Wolke JGC, Zhang D, de Groot K. The role of amorphous phase in nucleating bone-like apatite on plasma-sprayed hydroxyapatite coatings in simulated body fluid. *J Mater Sci Lett* 1997;16(4):335-337.
20. Kweh SW, Khor KA, Cheang P. Production and characterization of hydroxyapatite (HA) powders. *J Mater Process Technol* 1999;89-90:373-377.
21. Khor KA, Cheang P. Influence of powder characteristics on plasma sprayed hydroxyapatite coatings. *J Therm Spray Technol* 1996;5(3):310-316.
22. Tsui YC, Doyle C, Clyne TW. Plasma sprayed hydroxyapatite coatings on titanium substrates. Part I. Mechanical properties and residual stress levels. *Biomaterials* 1998;19:2015-2029.
23. McPherson R, Gane N. Structural characterization of plasma-sprayed hydroxyapatite coatings. *J Mater Sci Mater Med* 1995;6:327-334.
24. Sun L, Berndt CC, Lima RS, Kucuk A, Khor KA. Effects of spraying parameters on phase formation and distribution in plasma sprayed hydroxyapatite coatings. In: Berndt CC, editor. *Proceedings of International Thermal Spray Conference—ITSC2000*, May 8-11, 2000, Montreal, Canada. Materials Park, OH: ASM Int.; p 803-811.
25. Sun L, Berndt CC, Kucuk A, Lima RS, Khor KA. Surface characterization of plasma sprayed hydroxyapatite coatings. In: Jessen T, Ustundag E, editors. *Ceramic engineering and science proceedings. Proceedings of the 24th Annual Conference on Composites, Advanced Ceramics, Materials, and Structures: B*, 21(4), January 23-28, 2000, Cocoa Beach, FL. Westerville, OH: American Ceramic Society; p 251-258.
26. Koch B, Wolke JGC, de Groot K. X-ray diffraction studies on plasma-sprayed calcium phosphate-coated implants. *J Biomed Mater Res* 1990;24:655-667.
27. Ji H, Ponton CB, Marquis PM. Microstructural characterization of hydroxyapatite coating on titanium. *J Mater Sci Mater Med* 1992;3:283-287.
28. Lima RS, Kucuk A, Berndt CC. Evaluation of microhardness and elastic modulus of thermally sprayed nanostructured zirconia coatings. *Surf Coat Technol* 2001;135(2-3):166-172.
29. Matejcek J, Sampath S, Brand PC, Prask HJ. Quenching, thermal and residual stress in plasma sprayed deposits: NiCrAlY and YSZ coatings. *Acta Materialia* 1999;47(2):607-617.
30. Mancini CE, Berndt CC, Sun L, Kucuk A. Porosity determination of thermally sprayed hydroxyapatite coatings. *J Mater Sci* 2001;36(16):3891-3896.
31. Gross KA. Surface modification of biomedical prostheses. M.S. Thesis, Monash University, Australia. 1991.
32. Gross KA. The amorphous phases in hydroxyapatite coatings. Ph.D. Dissertation, AAI9616759. State University of New York at Stony Brook, Stony Brook, NY. 1995. p 175.
33. Radin SR, Ducheyne P. The effects of calcium phosphate ceramic composition and structure on *in vitro* behavior. II. Precipitation. *J Biomed Mater Res* 1993;27:35-45.
34. Tong W, Yang Z, Zhang X, Yang A, Feng J, Cao Y, Chen J. Studies on diffusion maximum in X-ray diffraction patterns of plasma-sprayed hydroxyapatite coatings. *J Biomed Mater Res* 1998;40:407-413.